Seasonal variability of tidal currents in Tampa Bay, Florida

Corresponding author: Gregory Dusek, Senior Scientist, Center for Operational Oceanographic Products and Services, National Ocean Service, NOAA, 1305 East West Hwy, Silver Spring, MD 20910 (gregory.dusek@noaa.gov)

Joseph Park, Scientist, South Florida Natural Resources Center, Everglades National Park, National Park Service, South Florida Natural Resources Center, 950 N Krome Ave, Homestead, FL 33030 (joseph_park@nps.gov)

Christopher Paternostro, Oceanographer, Center for Operational Oceanographic Products and Services, National Ocean Service, NOAA, 1305 East West Hwy, Silver Spring, MD 20910 (christopher.paternostro@noaa.gov)

Abstract

An analysis of tidal current variability is performed over seasonal scales for an 11-year record of estuarine currents at two locations in Tampa Bay, Florida. From 2002-2012 bi-monthly harmonic analyses are performed on current observations collected near the entrance to Old Tampa Bay and at Sunshine Skyway Bridge. The resultant tidal constituents and non-tidal residual are then correlated with other parameters to determine potential physical forcing. Comparison with local wind data suggests the land-sea breeze cycle can have significant impact on diurnal tidal current flow. Periods of strong land-sea breeze are found to have up to a 30% increase in K_1 amplitude compared to periods of weak land-sea breeze. Sub-tidal, weather scale wind forcing with periods from 2 to 7 days demonstrates strong correlation with non-tidal residual flow, likely resulting from both direct wind forcing as well as the modification of along-estuary water level gradients. Additionally, the M_2 constituent is found to be correlated with changes in freshwater discharge and inversely correlated with wind variance. The depth-averaged M_2 current amplitude can increase by more than 10 cm/s during periods of high discharge, representing a roughly 25% increase in the amplitude. The seasonal variability observed has significant impacts on the accuracy of tidal current predictions for marine navigation and other uses. Predictions of peak flood or ebb currents can vary by more than 40 cm/s depending on when observations are collected and when predictions are made.

INTRODUCTION

Research on estuarine currents is often limited to small-scale, short-period processes such as turbulence and mixing, or to large-scale, long-period estuarine circulation. In both cases tidal currents are typically

considered as secondary and do not receive attention outside of their influence on the process of interest. This may be partially attributed to the limited observational data of estuarine currents since in situ instrumentation (typically Acoustic Doppler Current Profilers or ADCPs) are often limited to deployments of a few months or less. Although it is known that tides (Flinchem and Jay 2000; Matte et al. 2013), and tidal currents (Visser et al. 1994) can be non-stationary due to non-tidal influences, tidal currents are often treated as stationary even though substantial variability will likely occur on seasonal time-scales, which is not captured over the length of a typical deployment.

Research regarding estuarine tidal seasonality has typically focused on water level measurements (Matte et al. 2013; Matte et al. 2014), where there are many long-term data sets (years to decades) available for analysis. There are relatively fewer examples of analyses regarding tidal current seasonality. Seasonal and spatial variability in tidal currents were examined in a portion of the Bering Sea (Danielson and Kowalik 2005), however observations were limited to about a year in duration. One of the longer records of estuarine currents is presented by Buijsman and Ridderinkhof (2007a, 2007b, 2008) in a series of papers, which include analyses of tidal, subtidal and secondary currents over five years of ferry-based ADCP observations. An examination of tidal currents was presented for the Strait of Gibralter for nearly six years of data (Sanchez-Roman et al. 2012), which may be the greatest duration of such an analysis in the peer-reviewed literature.

Despite a relative lack of long-term in situ observations, it has been well established that tidal currents vary seasonally. In regions of freshwater influence (ROFIs), it has been demonstrated through both numerical models and observations that tidal ellipses, in particular the M_2 tidal constituent, are influenced seasonally by freshwater discharge and the resultant stratification (Visser et al. 1994; de Boer et al. 2006; Palmer 2009) and mean outflow (Codiga and Rear 2002). Wind forcing from diurnal land/sea-breeze has been demonstrated to result in corresponding diurnal surface currents with

properties similar to diurnal tidal currents (Rosenfeld 1988; Hyder et al. 2002). Further, seasonal changes in diurnal winds have been shown to be the cause for seasonal variability in the K_1 tidal constituent (Alvarez et al. 2003). However, much of this research has focused on shelf regions and relies on relatively short duration observations and numerical models.

Perhaps the largest collection of long-term in situ current data is provided by the National Oceanic and Atmospheric Administration's (NOAA) Physical Oceanographic Real-Time System or PORTS®. PORTS® are collections of real-time sensors that measure a variety of coastal and estuarine phenomena including currents (Wolfe and MacFarland 2013). The primary purpose of PORTS® is to promote safe marine navigation, however PORTS® data are utilized for a wide range of research (Meyer et al., 2014), including circulation modeling (Wilson et al., 2006), seasonality in water level (Wahl et al., 2014) and Harmful Algal Bloom transport monitoring (Havens et al. 2010).

PORTS® with current observations of at least five years in duration include Chesapeake Bay, Delaware Bay, Galveston Bay, San Francisco Bay and others (tidesandcurrents.noaa.gov). The longest running PORTS® current measurements are collected at two locations in Tampa Bay which were installed initially in 1991 and since then have been operated fairly continuously. This data record coupled with the availability of additional physical oceanographic data and strong seasonal influences make Tampa Bay the ideal location for a seasonal analysis of tidal currents.

There are multiple benefits to better understanding tidal currents in Tampa Bay. On a local level this study yields insight into the physical processes of the Bay, and benefits other ongoing research on the Bay's circulation. On a broader level, better understanding temporal variability in tidal currents is of upmost importance to work that relies on the accurate prediction of tidal currents – for instance assessing hydrokinetic energy potential (Lanerolle et al. 2012), or predicting tidal currents for marine

navigation. The latter is of particular importance to the authors, as the NOAA National Ocean Service Center for Operational Oceanographic Products and Services (CO-OPS) is responsible for providing tidal current predictions at all heavily navigated coastal and estuarine regions in the United States. CO-OPS often relies on relatively short durations (~ months) of current observations to calculate tidal current predictions. This study seeks in part to determine the accuracy of tidal current predictions depending on when observations are collected. For example, tidal current predictions calculated from observations collected in the winter, may be much less accurate when applied during the summer months. The results have implications on how CO-OPS collects current observations and will have direct impact on the navigation community and marine safety.

This paper presents an examination of tidal current variability in Tampa Bay from 2002 to 2012. First a brief background on the physical oceanography of Tampa Bay is presented, followed by a presentation of methods including data collection, processing and analysis. This is followed by results including: the influence of wind on the K_1 constituent and residual energy, the impact of freshwater discharge and wind energy on the M_2 constituent, and implications of the temporal variability in tidal currents on the accuracy of tidal current predictions.

PHYSICAL SETTING

Tampa Bay is the largest estuary in Florida and in terms of tonnage, the 22nd largest of all ports in the United States (U.S. Army Corps of Engineers 2012). Tampa Bay can be classified as a drowned river valley and based on salinity distribution and stratification is considered partially to well-mixed (Weisberg and Zheng 2006). The length of the Bay is about 50 km, it has a variable width up to a maximum of about 15 km and an area just over 1,000 km^2 (Meyers and Luther 2008). Tampa Bay has an average depth of roughly 4 m (Goodwin 1987), with a deeper, narrow and dredged center navigation

channel that varies in depth from about 10 m to 25 m (Weisberg and Zheng 2006). Sediment input into the Bay from fluvial sources is quite low, and substantial transport of resuspended sediments has not been observed (Brooks and Doyle 1998). Although maintenance dredging in the Bay occurs fairly regularly, no large scale dredging projects have occurred in the two locations analyzed here (near Sunshine Skyway Bridge and at the entrance of Old Tampa Bay) from 2002 to 2012 (Mark Luther pers. comm.). As such, this analysis assumes changes in the bathymetry over the study period are minor and will not have any significant impact on the interpretation of the results. The watershed for the Bay is estimated at over 4,600 km^2 (Clark and MacAuley, 1989) with the largest freshwater input from the Hillsborough, Alafia, Little Manatee and Manatee Rivers.

Salinity is both spatially and seasonally dependent. During dry periods (typically later winter to spring months) surface salinity near the mouth of the Bay can be similar to what is found in the Gulf of Mexico (~35 psu), while surface salinity inland (near the entrance to Old Tampa Bay) may only be slightly lower (~30 psu). These dry periods also tend to exhibit greater vertical homogeneity and thus a weaker vertical salinity gradient (Meyers et al. 2007). Not surprisingly, during wet periods surface salinity tends to be lower throughout the estuary and can be closer to 25 psu at Sunshine Skyway near the mouth and 20 psu at Old Tampa Bay. Wet periods also tend to be more vertically stratified and have larger vertical salinity gradients (Meyers et al. 2007). Water temperature is seasonal, however tends to be more horizontally and vertically uniform than salinity (Zervas 1993). Relating the spatial gradients of temperature and salinity reveals that changes in density in the Bay are nearly entirely controlled by salinity (Meyers et al. 2015).

Tides and tidal currents in the Bay are of the mixed, mainly semidiurnal variety characterized by Defant ratios, D_r, between 0.5 and 1.5, defined as

$$D_r = \frac{K_1 + O_1}{M_2 + S_2}, \quad [1]$$

where each constituent represents the amplitudes along their major axis (Defant 1961; Zervas 1993). Tidal heights have D_r from 1.43 at Port Manatee near the entrance to 1.27 at Old Port Tampa and thus generally vary between one and two tides per day during any given month. The tidal currents were found to be more semi-diurnal with D_r from about 0.5 to 1 (Zervas 1993). Differences between tidal characteristics of water level and currents are not uncommon (Parker 2007). In this case, continuity requires that semi-diurnal transport rates (i.e., current amplitudes) are double that of diurnal transport rates, to transport roughly the same volume of water in half the time (Zervas 1993). The mean tidal range (the difference between mean high water and mean low water) for the Bay is fairly small and varies spatially from 35 cm to 55 cm, however the diurnal tidal range (the difference between mean higher high water and mean lower low water) is larger and varies from 67 to 76 cm. Mean flood and ebb currents are typically much faster within the channels (~ 50 cm/s – 75 cm/s) than in shallower regions (~ 10 cm/s; Zervas 1993).

Average non-tidal flow follows typical baroclinic estuarine circulation (Pritchard 1956), which is driven by horizontal salinity gradients from the head to the mouth of the Bay. This estuarine circulation is typified by fresher outflow to the Gulf at the surface and more saline inflow at depth. The average circulation is roughly an order of magnitude slower than tidal currents (< 10 cm/s; Weisberg and Zheng 2006; Meyers et al. 2007). Non-tidal circulation in the Bay is influenced by short-term factors like winds and freshwater input and was found to be significantly altered by extreme weather events like Hurricanes (Wilson et al. 2006). On seasonal scales, variability in freshwater input and vertical stratification has been shown to significantly alter Tampa Bay's subtidal circulation (Meyers et al. 2015). Circulation varies over longer time-scales due to changes in the bathymetry, human built infrastructure

like bridges (Meyers et al. 2013) or through climatic changes or cycles like ENSO (Schmidt and Luther, 2002).

METHODS

There were a variety of observational data sets utilized, with a majority of data collected at two locations: near the entrance to Tampa Bay at Sunshine Skyway Bridge, and near the entrance to Old Tampa Bay (Figure 1). The data collection, processing and analysis methodology for each data type is described below.

Currents

Currents data were collected from Teledyne RDI 1200 kHz Acoustic Doppler Current Profilers (ADCPs) deployed at both the Old Tampa Bay entrance and Sunshine Skyway Bridge (Figure 1). ADCPs were deployed at the bottom at both locations and provided 6 minute average currents over 1 m bins throughout the water column. The ADCP deployed at the Old Tampa Bay entrance is located at 27.863 N, 82.554 W, at approximately 12.75 m depth and referred to as Old Port Tampa (OP). At OP data were collected at 9 bin depths ranging from 10.8 m to 2.7 m. The ADCP deployed at Sunshine Skyway (SS) is located at 27.625 N, 82.655 W, at approximately 17 m depth. At SS data were collected at 11 bin depths ranging from 12.9 m to 2.9 m. The bins at 2.7 m and 2.9 m depth for OP and SS respectively were the closest to the surface with consistent quality data and are referred to as the near surface bin. ADCPs at both locations were initially installed in 1991 and have been maintained semi-continuously at relatively the same locations since. However, due to slight position changes and data availability the period used for analysis begins at April 15, 2002 for OP and April 12, 2004 for SS and continues until December 31, 2012 for both. Instruments received regular maintenance and data quality control occurred both in near real-time and via post-processing to ensure quality.

Harmonic analysis on currents data was performed using the MATLAB toolbox T_TIDE (Pawlowicz et al. 2002) based upon the least-squares harmonic analysis code originally developed by Foreman (1977). Harmonic analysis programs like T_TIDE model tidal response (water level or current) as:

$$x(t) = A_0 + \sum_{k=1}^{n} A_k \cos cos\,(\omega_k t - \varphi_k), \quad [2]$$

where A_0 is the mean (or residual) and A_k are unknown tidal constituent amplitudes with phase-shifts ϕ_k that are estimated for known constituent frequencies ω_k through a least-squares approach. The harmonic analysis was run for two-month (~61 day) partitions of *u* and *v* current velocity with 50% overlap, effectively providing monthly harmonic constituents (see Appendix for list of harmonic constituents). To account for missing data, the harmonic analysis results were only utilized if a given two-month period had at least 50% data density (Figure 2). A two-month duration was chosen to ensure sufficient data for an accurate harmonic analysis result, yet still provide reasonable seasonal resolution. Additional segment lengths and overlap percentages were tested, however largely yielded similar results.

The 61 day record length results in a minimum resolvable frequency of 0.0006 cph, which prevents resolving the Ss and Ssa constituents included in a long-term harmonic analysis. Further, the Rayleigh criterion, which dictates the ability to resolve constituents of similar frequency given the record length, precludes the inclusion of an additional 29 constituents which are solved for in a long-term harmonic analysis (see Appendix). Due to the Rayleigh criterion to separate P_1 from K_1 and K_2 from S_2 (186.2 days minimum record length) and the significance of the K_1 and S_2 constituents, a long-term harmonic analysis was run for the entire time period for both OP (11 years) and SS (9 years) to provide constituent values to infer P_1 and K_2 for the two-month harmonic analysis periods.

Water level

Six-minute water level data was collected via NOAA CO-OPS tide gauges at a nearly co-located station at OP, however for SS the nearest station was 9 km to the NE at Port Manatee (PM; Figure 1). Compared to currents data, water level had very little missing data, with data density of 97.2% (PM) and 88.5% (OP) over the entire 11 year period.

Harmonic analysis on water level data was performed using the NOAA CO-OPS harmonic analysis software based on the least-squares technique described in Harris et al. (1963) and later documented in Zervas (1999) and Parker (2007). A CO-OPS standard 37 constituents were calculated based on an average of four (OP) and five (PM) one-year harmonic analyses, and then used to calculate tidal predictions over the entire 11 year period (see Appendix). These predictions were then subtracted from observations to give a residual water level utilized in the analysis. This level of analysis was deemed sufficient for the water level data since only the long-term non-tidal residual is of interest in this study. The reduction of variance of the tidal constituents from the harmonic analysis of water levels, excluding the meteorologically-driven long period constituents, shows that the tidal constituents contribute to 64 – 65% of the total observed variance at Port Manatee and St. Petersburg, and about 74% at Old Port Tampa. Thus anywhere from 25 to 35% of the variance in water levels is due to non-tidal forces. This relatively large non-tidal component is due to the small tidal range, and the frequent contributions of subtidal wind events described later in this paper.

Other observations

Wind observations were co-located with the OP water level gauge and six-minute data were collected over the entire 11 year period with 77% data density. Only one source of wind data was utilized since previous work has shown that winds can generally be considered spatially homogeneous over Tampa Bay (Wilson et al. 2006). To allow comparison with the harmonic analysis results, the Power Spectral

Density (PSD) was computed for the wind data for the same bi-monthly sections if at least 75% of the six-minute wind samples were present for a given bi-monthly period. Linear interpolation was performed to fill missing observations prior to the PSD calculation.

Monthly-mean freshwater discharge was calculated from the nine most significant freshwater inputs into the Bay as measured by the United States Geological Survey (USGS; Table 1). These values were added to provide the total monthly-mean discharge into the Bay. Although total freshwater input to the Bay will also include direct precipitation and ungauged input sources, the estimate calculated from USGS gauges will provide a reasonable approximation of the monthly variability of the total freshwater input.

Water temperature and salinity data were collected by the Environmental Protection Commission of Hillsborough County (EPCHC) at many locations throughout the Bay as part of routine monitoring (wateratlas.usf.edu). The stations utilized here are those closest to OP (station 36) and SS (station 91) respectively (Figure 1). At each location data were collected on varying days, once a month at three depths. At OP the collection date was typically between the 1^{st}-10^{th} of each month and at SS the collection date was typically between the 20^{th} – 30^{th}. Since the lower two collection depths varied from month to month, and did not always capture the entire water column, only the surface salinity (~ 0.3 m depth) and the relative salinity gradient with depth are used to maintain consistency. These observations are primarily utilized as a supplemental data source due to the limited utility of spatially and temporally sparse data.

RESULTS

General observations

The results from the harmonic analysis show that currents at both OP and SS are predominantly tidal and have rectilinear along-channel flow. The tidal flow generally accounted for between 80-95% of the total variance for OP and SS, with total tidal energy decreasing with depth. The major axis (along-channel) component of the tidal flow generally accounted for at least 98% of the total variance for both stations. For this reason, this analysis is limited to the major axis tidal constituents (with the exception of the residual variance, which is the calculated from the magnitude of the major and minor axes).

The four largest tidal current constituents were M_2, S_2, K_1 and O_1 for both OP and SS (Table 2). Although error estimates for the constituent amplitudes are bin and time dependent, they are largely similar for the purposes of this analysis moving forward, and thus the mean error and one standard deviation are considered as an indicator of significance for the more detailed analysis of the M_2 and K_1 constituents. Mean error estimates for M_2 amplitudes are 2.02 cm/s (+- 0.45 sd) and 1.57 cm/s (+- 0.44 sd) for OP and SS respectively and for K_1 are 1.29 cm/s (+- 0.34 sd) and 1.48 cm/s (+-0.46 sd) for OP and SS respectively.

Average amplitudes for both locations were similar, with SS generally having slightly greater amplitudes for the near-surface bins than at OP. Unsurprisingly, phases for SS lead those of OP and there is relatively little variability with depth (Table 2). Generally the phases at depth slightly lead those at the surface for SS, due to the flood beginning with the inflow of bottom water. It is interesting to note that the diurnal phases at OP behave slightly differently and have the greatest lag at mid-depth. This is possibly due to the shallow water depth at OP and the potential for greater frictional and shallow-water effects. Despite this slight phase variability with depth, the resulting time differences are generally minor as a 5° change in phase represents only a 10 minute time difference for semidiurnal constituents and a 20 minute difference for diurnal constituents. There is also very little variability in the inclination

for all four major constituents due to the apparent topographically influenced rectilinear flow. The inclination at OP ranges from 20°-30° True (where 0° is True North) depending on time, constituent and depth and is essentially aligned with the channel. Similarly, SS inclination ranges from 50°-60° True and is also aligned with the channel at that location.

Wind influence

Analysis of the bi-monthly PSD results from the *u* and *v* wind components over the entire 11-year period indicates two main modes of wind variability influencing the Bay: The diurnal land-sea breeze cycle centered at about a 1 day period (and to a much lesser degree at a ½ day period); and the longer period weather driven wind events, ranging from periods of 2 to 30 days (Figure 3). The longer period weather events are more energetic in the *v* component, while the diurnal land-sea breeze is not surprisingly much more energetic in the *u* component (the coastline near the entrance of the Bay is close to N-S). These two characteristic modes were investigated for their influence on tidal current constituents and residual current energy.

Land-sea breeze cycle

To analyze the potential influence of land-sea breeze or diurnal winds on tidal constituents, the *u* and *v* components of the wind were translated to along- and cross-channel components for both OP (along-channel at 28°) and SS (along-channel at 57°). Bi-monthly PSDs of the along- and cross-channel wind components were calculated in the same manner as described previously and the variance from 0.95-1.05 cycles/day was calculated for each bi-monthly period. The analysis was insensitive to the precise frequency window utilized, and this range captured a vast majority of the diurnal energy. Yearly averaging over the entire analysis period shows diurnal winds to be most energetic in the late winter to spring months (Jan-May), which correlates well to the greatest K_1

amplitudes (Figure 4). At both OP and SS major axis K_1 amplitudes peak in the spring months from March to May and although the increase in amplitude is most significant near the surface, it extends well into the water column.

A scatter plot of the bi-monthly diurnal wind variance with the K_1 amplitude of the near surface bin at both OP and SS further indicates a relationship between wind forcing and K_1 (Figure 5). Both locations show increasing K_1 amplitudes related to increases in the diurnal wind variance, although with significant scatter (OP $r^2 = 0.22$, p-value = $< 1x10^{-4}$ and SS $r^2 = 0.33$, p-value $< 1x10^{-4}$). Differences in K_1 amplitude between time periods with negligible diurnal winds (variance < 0.2 $(m/s)^2$) and those with strong diurnal winds (variance ~ 1 $(m/s)^2$) can be about 3 cm/s for OP and 7 cm/s for SS. This represents roughly a 15% increase in K_1 amplitude for OP and a 30% increase for SS.

The agreement between the diurnal wind variance and the K_1 amplitudes suggests a regular, direct land-sea breeze forcing of the currents, which is then added to the astronomical K_1 tidal forcing. That SS is more significantly influenced than OP supports this conclusion, as the channel direction and major axis flow at SS (~ 57°) is much more aligned to the *u* wind component than at OP (28°). The phase of K_1 did not show a significant response to the increase in diurnal winds, nor did the O_1 amplitude or phase.

Long period wind variability

A majority of wind energy is found over periods ranging from 2 to 30 days, predominantly in the *v* component (Figure 3). This wind energy is spectrally much broader due to the natural variability of weather related wind impacts and consists of sub-tidal frequencies. It is expected that the influence of variable weather driven winds on currents will be part of the non-tidal residual current. A comparison of low-frequency wind energy with non-tidal residual reveals that both tend to be most significant in the

late fall to winter months (Nov – Feb), and during periods of significant tropical storms or hurricanes (Figure 6).

To determine at what frequency winds were most correlated to non-tidal residual energy, a regression is performed for each frequency band from 2 to 68 day periods with the depth-averaged fractional residual variance (i.e., the fraction of the total variance not captured by the harmonic analysis). The wind periods between 2 and 7 days demonstrated a significant relationship (positive slope) between wind and residual energy and were on average more correlated than at longer periods. In addition, it was found that the *v* component of the wind correlated more closely with the fractional residual variance (SS r^2 = 0.21, p-value = 1.3×10^{-4}; OP r^2 = 0.59, p-value < 1×10^{-4}) than the *u* component (SS r^2 = 0.13, p-value = 3.5×10^{-3}, OP r^2 = 0.28, p-value < 1×10^{-4}) and was comparable to the along-channel component (SS r^2 = 0.19, p-value = 3.9×10^{-4}; OP r^2 = 0.61, p-value < 1×10^{-4}) . A visual comparison also indicates that the depth-averaged fractional residual variance demonstrates a slight relationship with the 2-7 day wind variance at SS, however is better correlated at OP (Figure 7). In both cases the trend is such that an increase in lower frequency wind variance can lead to substantially greater residual current variance (~ 10% greater residual variance for OP).

A strong correlation with the *v* component of the wind suggests that longer period wind forcing may be influencing currents indirectly, through along channel water level gradients. N-S winds may be resulting in net transport into or out of the Bay, driving variations in water level, which result in greater non-tidal current energy. To determine the relationship between winds and residual (non-tidal) water level, squared coherence over the same bi-monthly periods was calculated, where squared coherence following Emery and Thomson (2004) is defined as:

$$C_{w\eta}^2 = \frac{\left|G_{w\eta}(f_k)\right|^2}{G_{ww}(f_k)G_{\eta\eta}(f_k)}, \quad [3]$$

where G_{ww} is the autospectrum for the wind, $G_{\eta\eta}$ is the residual water level autospectrum and $G_{w\eta}$ is the cross-spectrum for each frequency f_k . The squared coherence between the bi-monthly water level residual at both OP and PM (nearest station to SS) and the wind observations demonstrates a strong relationship at low frequencies (Figure 8). In particular the *v* component of the wind is highly coherent with lower frequency water level residual at OP, with peak coherence of 0.81 at about 7 days. Although qualitatively similar, the low-frequency coherence is slightly greater for OP than for SS. These results indicate a strong relationship between the 2-7 day period winds and water level, clearly establishing wind forcing of water level as a forcing mechanism for sub-tidal residual currents. Comparisons between bi-monthly mean wind energy and water level residual were also made, however no significant relationship was found.

Freshwater discharge and stratification

Precipitation and freshwater discharge into Tampa Bay tends to peak in the late summer and early fall months (July – October), and similarly the M_2 current amplitude increases during these time periods (Figure 9). This suggests a relationship between increased discharge, greater freshwater content in the Bay and the amplitude of the M_2 constituent. The long period harmonic constituents (Sa and Ssa) are often associated with seasonal variability, and cannot be calculated with a 2 month time series. The Sa and Ssa amplitudes for the long-term harmonic analysis are 1.18 cm/s and 0.46 cm/s respectively for OP and 1.27 cm/s and 0.70 cm/s for SS. That these amplitudes are insignificant relative to the variability observed in M_2 ensures that an artificial seasonal variation in the M_2 is not being included by excluding these constituents.

Correlations were computed using various combinations of the M_2 amplitude and the mean monthly discharge, however the greatest correlation was found between the depth-averaged bi-monthly M_2

amplitude and the mean monthly discharge averaged for the previous and present month (Figure 10). This relationship is sensible because the bi-monthly harmonic analysis period extends into the previous month (e.g., harmonic analysis is from March 15 –May 15 and discharge is from March 1-April 30), and also because freshwater discharge will have some residence time in the Bay (estimated to be on average between 26-53 days depending on freshwater inflow; Meyers and Luther 2008).

The best regression fit between the M_2 amplitude and discharge was found to be non-linear of the form $A(1 - e^{bx})$, and has r^2 values of 0.47 and 0.46 (p-value < $1x10^{-4}$) for OP and SS respectively compared to 0.41 and 0.42 (p-value < $1x10^{-4}$) for the linear fit. Further it was found that the M_2 amplitude is inversely correlated with wind energy and by including the bi-monthly v wind variance as an additional predictor in a multiple linear regression, the fit is improved significantly for both OP and SS (r^2 of 0.68 for both; p-value < $1x10^{-4}$). Interpreting the plots, it is evident that there is significant variability in the M_2 amplitude at lower discharge levels (< 20 m^3/s), which suggests other factors such as wind energy alter the M_2 amplitude at these low levels. At high discharge levels, there is less variability evident and an apparent saturation of the M_2 amplitude. During periods of high discharge the M_2 amplitudes of both OP and SS are about 10 cm/s greater than average conditions at low discharge, which is roughly a 25% increase in amplitude. The relationship between the M_2 amplitude, freshwater discharge and wind energy suggests that increased stratification may be contributing to the increase in the M_2amplitudes.

A relationship between monthly mean discharge, surface salinity and the salinity gradient at both OP and SS supports the likelihood that stratification is influencing the M_2 amplitudes. There is very good agreement in salinity variability between OP and SS as evident in Figure 11, and with a normalized cross correlation of 0.85 (all coefficients with 95% confidence bounds of $\pm$ 0.17). Not surprisingly, surface salinity is also highly inversely correlated with mean discharge. The correlation coefficient between discharge and surface salinity at zero lag was found to be -0.73 at OP and -0.64 at SS.

Interestingly, at both locations there was also a high inverse correlation at one-month lag (-0.68 at OP, -0.66 at SS) and at a two-month lag (-0.46 at OP, -0.48 at SS). It is important to recall that the salinity measurements are made at an instant in time each month, while the discharge is a monthly mean value. Although part of the lag correlation is likely due to the timing of the salinity samples compared to the discharge measurements, some of the lag is undoubtedly due to the residence time of the freshwater in the system and points to why the relationship between M_2 and discharge is better estimated by examining present and previous months of discharge combined.

The salinity gradient estimated by CTD casts tends to increase during periods of increased discharge as well (Figure 11c), and this points to a potential increase in stratification (acknowledging that the casts are just an instant in time). Further, during these periods of increased discharge, surface salinity and stratification the mean along-channel current at SS shows increased inflow throughout most of the water column (Figure 11d). This increase in inflow indicates greater exchange with the Gulf during these same periods.

Implications on tidal current predictions

An analysis of tidal current predictions generated from each bi-monthly set of tidal constituents was performed to assess how seasonal differences in constituents influence the accuracy of the predictions. Predictions were generated from each bi-monthly period (127 periods for OP and 103 for SS) and each time series of predictions cover the entire analysis period. The total residual variance and fractional residual variance were then calculated for each month there were observed data available. The results of this analysis find that for a given month of observations, the amount of variance (i.e., the current energy not predicted) could vary substantially (> 25%) depending on what bi-monthly constituents were used to generate the predictions.

An example for this is shown for January 2006 for both OP and SS (Figure 12). In this case the fraction of residual variance is shown for January 2006, when each bi-monthly period of constituents are utilized. Not surprisingly, the lowest amount of residual variance (OP = 0.14 and SS = 0.12) was found when the predictions were generated from the same bi-monthly period centered on January 2006. In general, the predictions generated from observations collected during the winter months of each year (Dec – Jan) are the most accurate, or have the lowest residual variance. For the winter months the difference in variance is always less than 0.04 for SS and less than 0.10 for OP. When predictions are generated from observations during the spring (when K_1 generally increases) or the early Fall (when M_2 generally increases) the amount of residual variance can increase dramatically. In the case of SS it can often reach a 0.10 increase, and for OP the variance increases in excess of 0.20 in multiple instances (Figure 12). This magnitude of increased residual variance or "error" in the tidal current predictions tends to behave similarly when comparing other seasonally different time periods throughout the 11-year analysis.

DISCUSSION AND CONCLUSION

A harmonic analysis of 11 years of ADCP data collected at two locations in Tampa Bay show that the M_2 and K_1 tidal current constituents as well as the non-tidal residual current have significant seasonal variability. The observed seasonality is driven by changes in wind forcing and freshwater input. This variability in tidal current constituents strongly influences tidal current predictions generated from short-term observations depending on the observed and predicted time periods.

There are two primary modes of wind variability at Tampa Bay: a diurnal land-sea breeze cycle that is predominantly observed in the *u* wind component, and sub-tidal winds driven by changing weather patterns more energetic in the *v* wind component. Wind stress from the diurnal land-sea breeze likely

forces currents directly, which are then observed in the harmonic analysis as a component of the K_1 tidal constituent due to the similar frequency of the land-sea breeze and astronomical forcing. Although there is a clear trend of increasing K_1 amplitudes for both the OP and SS locations with increasing diurnal wind energy, there is significant scatter in data with low resultant correlation. Also, although the diurnal wind energy is significant and fairly consistent from January to May (Figure 4), the response by the K_1 amplitude does not typically reach a maximum until April. This is suspected to be related to the timing of the land-sea breeze cycle compared to the phase of the K_1 constituent. The shorter daylight in January (~10.5 hours) and February (~11 hours) preclude a precise alignment between the diurnal winds and the K_1 tidal current for both the flood and ebb cycles. Whereas in March and April, the day/night cycle is closer to a 12 hour split, thus leading to a more regular land-sea breeze with both onshore and offshore components in phase with the K_1 constituent.

The lower frequency weather related winds are well correlated with the variance of the non-tidal residual current. Specifically, the *v* component of the wind with a periodicity between 2 and 7 days demonstrates the greatest correlation with the residual current variance. The *v* component was found to be highly correlated with changes in water level at both OP and PM, with a peak correlation at 7 days (Figure 8). This correlation with water level suggests why this type of wind forcing strongly influences residual currents. Southerly winds along the coast increase transport into the Bay, causing an increase in water level. The Bay's north-south orientation also leads to southerly winds providing increased transport to the northern portion of the Bay further increasing water level in Old Tampa Bay (near OP). Once the southerly winds relax (or change orientation) the water pushed into the northern portion of the Bay returns southward and exits the Bay, decreasing water levels. The sub-tidal currents are forced both directly by the winds, but also influenced by the change in the along-estuary water level gradients from onshore and up-estuary transport. Although this type of sub-tidal residual flow does not directly

influence tidal current constituents, the increase in residual currents will increase the amount of "error" when relying on tidal current predictions and thus are important to consider when determining the reliability of such predictions.

The variability of the M_2 tidal constituent is found to be nonlinearly dependent on freshwater discharge and inversely correlated to *v* wind variance. The increase in depth-averaged M_2 amplitude can exceed 10 cm/s during periods of high discharge, which represents a roughly 25% increase in amplitude compared to periods of low discharge. In addition to an increase in M_2 amplitude throughout the water column, the vertical gradient in M_2 amplitude tends to increase and deepen. The increase in M_2 amplitude and stronger vertical gradient occurs predominantly in the summer months, when freshwater input is greatest and wind energy is generally low.

The relationship of the M_2 constituent to both freshwater discharge and wind energy, suggests both increased outflow and increased stratification as a potential mechanisms for greater M_2 amplitudes. During periods of high discharge, there will be increased outflow, and thus increased inflow and exchange with the Gulf (Figure 11d). This increase in subtidal circulation has been demonstrated to occur in Tampa Bay during the Fall months, where peak outflow reaches 20 cm/s (Myers et al. 2015). It is reasonable to expect that since M_2 is the largest tidal current constituent, the greatest increase in exchange will occur over the M_2 cycle.

During the summer months, the increase in freshwater input coupled with decreased mixing due to low wind energy would support more stratified conditions. This hypothesis is supported by the strong correlation between discharge and surface salinity at both OP and SS, coupled with an increase in the observed salinity gradient during these periods (Figure 11). Interestingly, there are some periods in the winter and early spring months where there is increased discharge (e.g., December 2002; Figure 9), yet

the M_2 amplitude does not increase as greatly as in the summer months. These periods tend to have greater wind energy and are likely less stratified, which demonstrates the combined significance of both discharge and wind energy and that discharge alone is not the mechanism for increased M_2 amplitudes.

Periods of increased stratification could potentially enhance this flow for two reasons. Increased stratification will result in reduced eddy viscosity and limit mixing between the surface and at depth. Myers et al. (2015) show that increased stratification in the Fall months may be a driver for the aforementioned increase in observed subtidal flow and thus exchange. In addition, the increased baroclinicity will decrease the frictional dissipation of the tidal current in the surface layers thus increasing vertical variability, an effect observed and modeled in previous research of Tampa Bay (Arnott et al. 2012). Whereas a more homogeneous water column would lead to a more barotropic tidal current and cause frictional dissipation to more greatly influence the entire water column.

The implications of seasonality in tidal currents are evident when comparing tidal current predictions generated from different bi-monthly periods. There were instances of an increase in the residual variance (e.g., current not predicted) of over 10% for SS and 20% for OP depending on what observations were used to generate the tidal current predictions (Figure 12). This result portends a real-world impact of this seasonality.

The marine navigation community relies on tidal current predictions for safe navigation. Most often the times and magnitudes of maximum flood and ebb currents are utilized by navigators, and in some cases as threshold values to determine time periods for safe navigation. Maximum flood and ebb currents can often reach 80 cm/s at OP and 100 cm/s at SS. For the example cited above and in Figure 12, using predictions generated from data in the Fall compared to predictions generated from observations in January, results in differences of 20-30 cm/s for the magnitude of maximum flood or ebb at OP. For SS,

although the relative change in residual is lower, since the maximum currents are faster – a similar comparison results in differences of 40 cm/s or more, especially during Spring tides. In both cases these differences are substantial, and could have significant impact on achieving effective and safe navigation.

This study provides an examination of tidal currents for one of the longest continuous records of estuarine current observations presently available. The results presented here suggest that an assumption of stationarity in tidal currents is not reasonable in some estuarine areas. It is standard practice to utilize one to two months of data to generate indefinite tidal current predictions for a particular location. This length of observation may not be sufficient to accurately resolve tidal currents in some locations, and a different sampling strategy may need to be considered. The results here also point to the importance of obtaining long data sets of current observations in estuarine areas which capture seasonal variability. This type of seasonal analysis would not be possible without multiple years of nearly continuous observations. Lastly, this study provides important insight in tidal flow and the physical processes of Tampa Bay. Future work may include a similar examination at other long term current observations collected at NOAA PORTS® locations like Delaware Bay and Chesapeake Bay, as well as further investigation of the relationship between tidal currents and other physical processes of Tampa Bay through a numerical model.

APPENDIX: Tidal constituents utilized in harmonic analysis

Due to the varying data record lengths utilized in the harmonic analyses, different tidal constituents were solved for in the analysis of the long term currents, bi-monthly currents and water level. The constituents included in each type of harmonic analysis are as follows.

Constituent	Frequency (cph)	Long term currents	Bi-monthly currents	Water level
Sa	0.0001	X		X
Ssa	0.0002	X		X
Msm	0.0013	X		
Mm	0.0015	X	X	X
MSf	0.0028	X	X	X
Mf	0.0031	X		X
α1	0.0344	X	X	
2Q1	0.0357	X	X	X
σ1	0.0359	X		
Q1	0.0372	X	X	X
ρ1	0.0374	X		X
O1	0.0387	X	X	X
τ1	0.0390	X		
β1	0.0400	X		
M1	0.0403	X	X	X
χ1	0.0405	X		
π1	0.0414	X		
P1	0.0416	X	X	X
S1	0.0417	X		X
K1	0.0418	X	X	X
ψ1	0.0419	X		
φ1	0.0420	X		
θ1	0.0431	X		
J1	0.0433	X	X	X
SO1	0.0446	X		
OO1	0.0448	X	X	X
υ1	0.0463	X	X	
OQ2	0.0760	X		
ε2	0.0762	X	X	
2N2	0.0775	X		X
μ2	0.0777	X	X	X
N2	0.0790	X	X	X
ν2	0.0792	X		X
Γ2	0.0803	X		
H1	0.0804	X		

M2	0.0805	X	X	X
H2	0.0806	X		
MKS2	0.0807	X		
λ2	0.0818	X		X
L2	0.0820	X	X	X
T2	0.0832	X		X
S2	0.0833	X	X	X
R2	0.0834	X		X
K2	0.0836	X	X	X
MSN2	0.0848	X		
η2	0.0851	X	X	
2SM2	0.0862			X
MO3	0.1192	X	X	X
M3	0.1208	X	X	X
SO3	0.1221	X		
MK3	0.1223	X	X	X
SK3	0.1251	X	X	
MN4	0.1595	X	X	X
M4	0.1610	X	X	X
SN4	0.1623	X	X	
MS4	0.1638	X	X	X
MK4	0.1641	X		
S4	0.1667	X	X	X
SK4	0.1669	X		
2MK5	0.2028	X	X	
2SK5	0.2084	X	X	
2MN6	0.2400	X	X	
M6	0.2415	X	X	X
2MS6	0.2444	X	X	
2MK6	0.2446	X		
2SM6	0.2472	X	X	
MSK6	0.2474	X		
S6	0.2500			X
3MK7	0.2833	X	X	
M8	0.3220	X	X	X
Total solved for		**68**	**37**	**37**

ACKNOWLEDGEMENTS

The authors would like to thank Armin Pruessner, Paul Fanelli and Colleen Fanelli for their assistance with data retrieval. We would also like to thank Stephen Gill, Chris Zervas, Lyon Lanerolle and three anonymous reviewers for their review and feedback.

All current, water level and wind data used for this research is freely accessible online and can be found at tidesandcurrents.noaa.gov. Discharge data is available through the USGS at: waterdata.usgs.gov. Water temperature and salinity data is available at: wateratlas.usf.edu.

REFERENCES

Alvarez, O., Tejedor, B., Tejedor, L. and B.A. Kagan (2003). "A note on the sea-breeze-induced seasonal variability in the K1 tidal constants in Cadiz Bay, Spain." Estuarine, Coastal and Shelf Science, 58(2003), 805-812.

Arnott, K.D., Valle-Levinson, A. and M. Luther (2012). "Friction dominated exchange in a Florida estuary." Estuarine, Coastal and Shelf Science. 113, 248-258.

Brooks, G.R. and L.J. Doyle (1998). "Recent sedimentary development of Tampa Bay, Florida: A microtidal estuary incised into tertiary platform carbonates" Estuaries 21(3), 391-406.

Buijsman, M. C. and H. Ridderinkhof (2007a). "Long-term ferry-ADCP observations of tidal currents in the Marsdiep Inlet." Journal of Sea Research, 57(2007), 237-256

Buijsman, M. C. and H. Ridderinkhof (2007b). "Water transport at subtidal frequencies in the Marsdiep inlet." Journal of Sea Research, 58(2007), 255-268

Buijsman, M. and H. Ridderinkhof (2008). "Variability of secondary currents in a weakly stratified tidal inlet with low curvature." Continental Shelf Research, 28, 1711 – 1723

Clark, P.A. and R.W. MacAuley (1989). "Geography and economy of Tampa Bay and Sarasota Bays." In: Tampa and Sarasota Bays: Issues, Resources, Status, and Management. *NOAA Estuary-of-the-Month Seminar Series No. 11,* 1-17.

Codiga, D.L. and L.V. Rear (2004). "Observed tidal currents outside Block Island Sound: Offshore decay and effects of estuarine outflow." Journal of Geophys. Res., 109, C07S05, doi: 10.1029/2003JC001804.

Danielson, S. and Z. Kowalik (2005). "Tidal currents in the St. Lawrence Island region." *J. Geophys. Res.,* 110., C10004, doi: 10.1029/2004JC002463.

de Boer, G.J., Pietrzak, J.D. and J.C. Winterwerp (2006). "On the vertical structure of the Rhine region of freshwater influence." Ocean Dynamics, 56, 198-216.

Defant, A. (1961). Physical Oceanography, Vol. 2, Pergamon Press, New York, NY, 598 pp.

Emery, W.J. and R.E. Thomson (2004). Data analysis methods in physical oceanography: Second and revised edition. Elsevier B.V., Amsterdam, Netherlands. 638 pp.

Flinchem, E.P. and D.A. Jay (2000). "An introduction to wavelet transform tidal analysis methods." *Estuarine, Coastal and Shelf Science, 51,* 177-200. doi:10.1006/ecss.2000.0586.

Foreman, M.G.G. (1977). "Manual for tidal heights analysis and prediction." *Pacific Marine Science Report 77-10,* Institute of Ocean Sciences, Patricia Bay, Sidney, BC, 97 pp.

Goodwin, C.R. (1987). "Tidal-flow, circulation, and flushing changes caused by dredge and fill in Tampa Bay, Florida." *U.S. Geological Survey Water-Supply Paper 2282*, 25 pp.

Harris, D.L., N.A. Pore and R. Cummings (1963). "The application of high speed computers to practical tidal problems." Abstracts of Papers, vol 6, IAPO, XIII General Assembly, IUGG, Berkely, VI-16.

Havens, H., M.E. Luther, S.D. Meyers and C.A. Heil (2010). "Lagrangian particle tracking of a toxic dinoflagellate bloom within the Tampa Bay estuary." *Mar. Pollut. Bull., 60(12),* 2233-2241.

Hyder, P., Simpson, J.H. and S. Christopoulos (2002). "Sea-breeze forced diurnal surface currents in the Thermaikos Gulf, North-west Aegean." Continental Shelf Research, 22(2002), 585-601.

Lanerolle, L.W.J., Paternostro, C., Dusek, G. and Rear-McLauglin, L. (2012). "An assessment of the renewable hydrokinetic energy potential in Cook Inlet, Alaska." *Proceedings of MTS/IEE Oceans 2012, Hampton Roads, VA.*

Matt, P., D.A. Jay and E.D. Zaron (2013). "Adaptation of classical tidal harmonic analysis to nonstationary tides, with application to river tides." *J. Atmos. Ocean Tech., 30,* 569-589. doi: 10.1175/JTECH-D-12-000016.1.

Matte, P., Y. Secretan and J. Morin (2014). "Temporal and spatial variability of tidal-fluvial dynamics in the St. Lawrence fluvial estuary: An application of nonstationary tidal harmonic analysis." *J. Geophys. Res., 119*, doi: 10.1002/2014JC009791.

Meyers, S.D., M.E. Luther, M. Wilson, H. Havens, A. Linville, and K. Sopkin (2007). "A numerical simulation of residual circulation in Tampa Bay. Part 1: Low-frequency temporal variations." *Estuaries and Coasts, 30(4)*, 679-697.

Meyers, S.D and M.E. Luther (2008). "A numerical simulation of residual circulation in Tampa Bay. Part 2: Lagrangian residence time." *Estuaries and Coasts, 31*, doi: 10.1007/s12237-008-9085-0.

Meyers, S.D., A.J. Linville and M.E. Luther (2013). "Alteration of residual circulation due to large-scale infrastructure in a coastal plain estuary." *Estuaries and Coasts,* doi: 10.1007/s12237-013-9691-3.

Meyers, S.D., J. Scudder and M.E. Luther (2014). "Real-time oceanographic data: From safety to science." *Eos Trans. AGU, 95(34),* 305-306.

Meyers, S.D., M. Wilson and M.E. Luther (2015). "Observations of hysteresis in the annual exchange circulation of a large microtidal estuary." *J. Geophys. Res. Oceans, 120,* 2904-2919, doi: 10.1002/2014JC010342.

Palmer, M.R. (2009). "The modification of current ellipses by stratification in the Liverpool Bay ROFI." Ocean Dynamics, 60, 219-226.

Parker, B. (2007). Tidal analysis and prediction, NOAA Special Publication NOS CO-OPS 3. Silver Spring, MD.

Pritchard, D.W. (1956). "The dynamic structure of a coastal plain estuary." *Journal of Marine Research, 15,* 33-42.

Pawlowicz, R., B. Beardsley and S. Lentz (2002). "Classical tidal harmonic analysis including error estimates in MATLAB using T_Tide." *Computers and Geosciences, 28,* 929-937.

Rosenfeld, L.K. (1988). "Diurnal period wind stress and current fluctuations over the continental shelf off Northern California." Journal of Geophys. Res., 93, 2257-2276.

Sanchez-Roman, A., J. Garcia-Lafuente, J. Delgado, J.C. Sanchez-Garrido and C. Naranjo (2012). "Spatial and temporal variability of tidal flow in the Strait of Gibraltar." *Journal of Marine Systems, 98-99*, doi: 10.106/j.jmarsys.2012.02.011.

Schmidt, N. and M.E. Luther (2002). "ENSO impacts on salinity in Tampa Bay, Florida." *Estuaries, 25(5),* 976-984.

US Army Corps of Engineers (2012). Waterborne commerce of the United States: Calendar Year 2012, Part 5- National Summaries. USACE Institute for Water Resources, Alexandria, VA.

Visser, A.W., Souza, A.J., Hessner, K. and J.H. Simpson (1994). "The effect of stratification on tidal current profiles in a region of freshwater influence." Oceanologica, 17(4), 369-381.

Wahl, T., F.M. Calafat and M.E. Luther (2014). "Rapid changes in the seasonal sea level cycle along the US Gulf coast from the late 20th century." *Geophys. Res. Lett., 41,* 491-498, doi:10.1029/2013GL058777.

Weisberg, R.H. and L. Zheng (2006). "Circulation of Tampa Bay driven by buoyancy, tides and winds, as simulated using a finite volume coastal ocean model." *J. Geophys. Res., 111,* C01005, doi:10.1029/2005JC003067.

Wilson, M., S.D. Meyers and M.E. Luther (2006). "Changes in the circulation of Tampa Bay due to Hurricane Frances as recorded by ADCP measurements and reproduced with a numerical ocean model." *Estuaries and Coasts, 29(6A),* 914-918.

Wolfe, K.E. and D. MacFarland (2013). An assessment of the value of the Physical Oceanographic Real-Time System (PORTS®) to the U.S. Economy. National Ocean Service, NOAA, Silver Spring, MD, 500pp.

Zervas, C.E.E. (1993). Tampa Bay oceanography project: physical oceanographic synthesis, NOAA Technical Report NOS OES 002. Office of Ocean and Earth Sciences, Silver Spring, MD. 184 pp.

Zervas, C.E.E. (1999). Tidal current analysis procedures and associated computer programs. NOAA Technical Report NOS CO-OPS 0021. National Ocean Service, NOAA, Silver Spring, MD. 101 pp.

Table 1. USGS gauges utilized for calculating total freshwater discharge into Tampa Bay

Station	USGS ID
Alafia River	02301500
Bullfrog Creek	02300700
Hillsborough River	02304500
Lake Tarpon Canal	02307498
Little Manatee River	02300500
Manatee River	02299950
Rocky Creek	02307000
Saltwater Creek	02306647
Ward Lake	02300042

Table 2. Bi-monthly average major axis amplitudes (cm/s) and phases (degrees) for the four largest tidal current constituents, and average amplitudes (cm) and phases (degrees) for the same water level tidal constituents

Constituent	Old Port Tampa						Sunshine Skyway / Port Manatee					
	Bottom Current		Surface Current		Water Level		Bottom Current		Surface Current		Water Level	
	Amp	Pha	Amp	Pha	Amp	Pha	Amp	Pha	Amp	Pha	Amp	Pha
M_2	34.5	147	44.9	150	20	215	31.3	121	49.4	125	16.1	172
S_2	11.3	169	14.4	170	6.3	234	11.3	140	16.9	140	5.5	187
K_1	16.1	337	21.1	323	17.6	57	17.4	326	27.3	330	16.0	40
O_1	13.8	324	18.1	336	15.9	44	15.1	313	23.8	317	14.8	27

Figure Captions

Figure 1. Map showing the study area. Locations of ADCPs , water level gauges and CTD measurements are shown. Circles designate the Old Port Tampa site and squares show the Sunshine Skyway site. Wind data is co-located with the Old Port Tampa water level gauge.

Figure 2. Bars indicate months in which sufficient ADCP current data was collected to run a harmonic analysis (> 50% data density) from 2002 to 2012. Both Old Port Tampa (black) and Sunshine Skyway (gray) are shown.

Figure 3. Mean of the bi-monthly PSD of the *u* and *v* wind velocity. Spectral peaks show long period weather driven events under 0.5 cycles/day and the diurnal land-sea breeze cycle at 1 and 2 cycles/day. 95% confidence limits are shown (dashed lines).

Figure 4. Average bi-monthly diurnal wind variance of the along-channel wind component (OP at 28° and SS at 57°), plotted over the average bimonthly major axis K_1 amplitude. Averages are made over the entire analysis period for both OP (2002-2012) and SS (2004-2012).

Figure 5. Diurnal wind variance of the along-channel wind component (OP at 28° and SS at 57°) and the major axis K_1 amplitude at the near surface bin for OP (black) and SS (white). Lines indicate best fit linear trend.

Figure 6. The contour plots show OP (A) and SS (B) non-tidal residual variance with depth (left y-axis), going from 2002 (top) to 2012 (bottom). The black line shows the corresponding bi-monthly

low frequency wind (2 to 30 day period) variance (right y-axis) over the same time period. Months with dramatically larger residual variance indicate large tropical storm events (e.g. Sep. 2004).

Figure 7. Wind variance of the *v* component from periods of 2 to 7 days and the depth averaged fractional residual variance from both OP (black) and SS (white) for each bi-monthly period over the analysis period. Lines indicate best fit linear trend.

Figure 8. Average squared coherence between *v* (solid) and *u* (dashed) wind component and residual water level at OP and PM is shown. Squared coherence estimates were made for each bi-monthly period and then averaged over the entire analysis period. The 95% confidence limit for this coherence function assuming 8.8 equivalent degrees of freedom is 0.32.

Figure 9. The contour plots show OP (A) and SS (B) M_2 major axis amplitude with depth (left y-axis), going from 2002 (top) to 2012 (bottom). The black line shows mean monthly discharge rate into Tampa Bay (right y-axis) over the same time period.

Figure 10. Bi-monthly mean discharge rate into Tampa Bay (A), bi-monthly *v* wind variance (B) and the depth-averaged major axis M_2 amplitude for OP (black) and SS (white). The bi-monthly discharge average is over the previous and concurrent month to the M_2 amplitude calculations. Lines indicate best fit non-linear trend for discharge and linear trend for wind.

Figure 11. Mean monthly discharge rate for Tampa Bay (A), the OP (solid) and SS (dashed) surface salinity (B) and salinity gradient (C), and the bimonthly mean along-channel current for SS (D). Positive mean current values indicate a current into the Bay.

Figure 12. The fractional residual variance for current observations from January 2006, when tidal current predictions are generated from bi-monthly harmonic analysis of each month and year shown for both OP and SS. Bar height shows the fractional residual variance for predictions from a particular month and year (leftmost/darkest bar - 2002 to rightmost/lightest bar 2012). The black arrow shows residual variance for predictions generated from the bi-monthly harmonic analysis centered in January 2006.

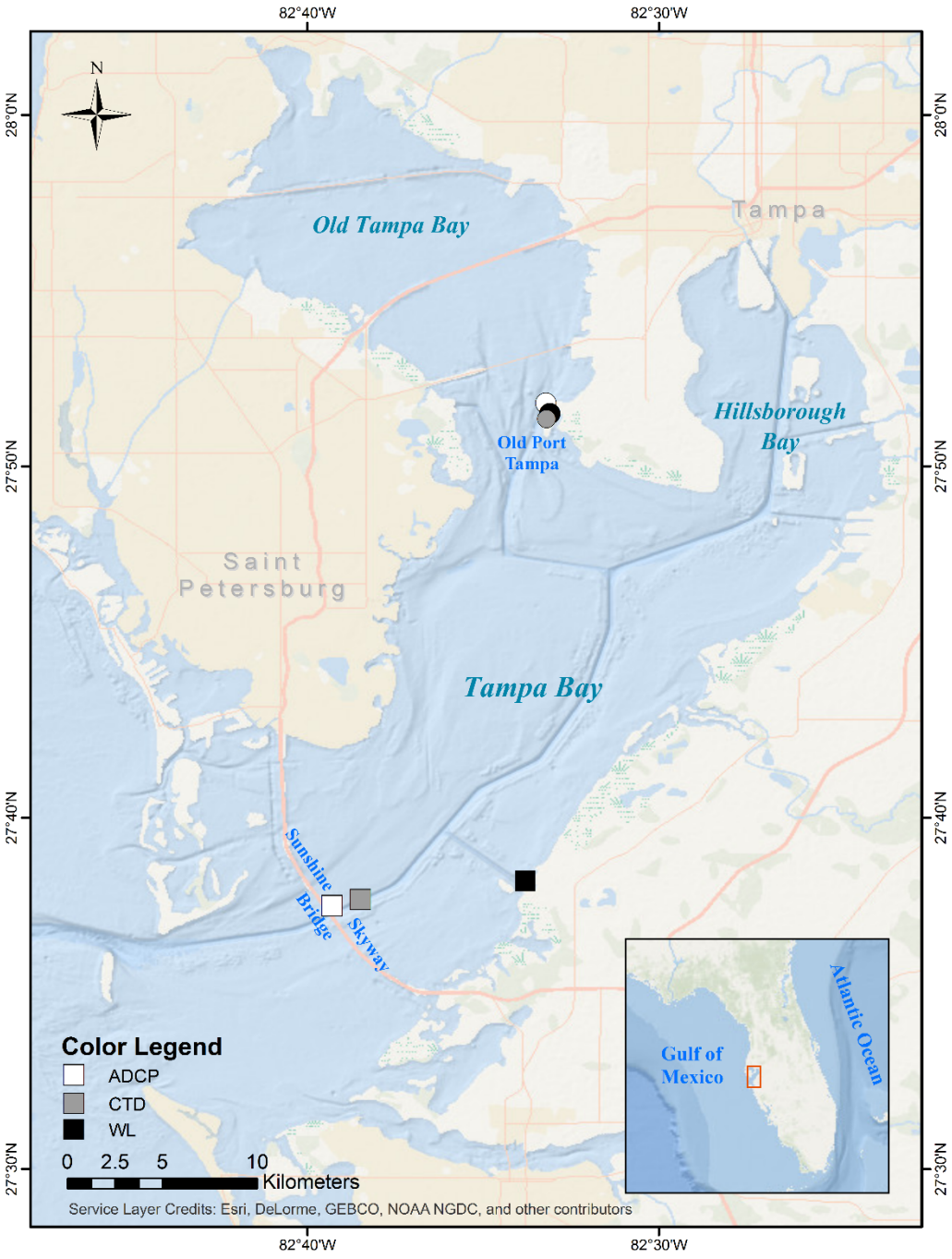
82°40'W
82°30'W
28°0'N
27°50'N
27°40'N
27°30'N
N
Old Tampa Bay
Tampa
Hillsborough Bay
Old Port Tampa
Saint Petersburg
Tampa Bay
Sunshine Skyway Bridge
Color Legend
ADCP
CTD
WL
0 2.5 5 10
Kilometers
Service Layer Credits: Esri, DeLorme, GEBCO, NOAA NGDC, and other contributors
Gulf of Mexico
Atlantic Ocean

Figure 1.

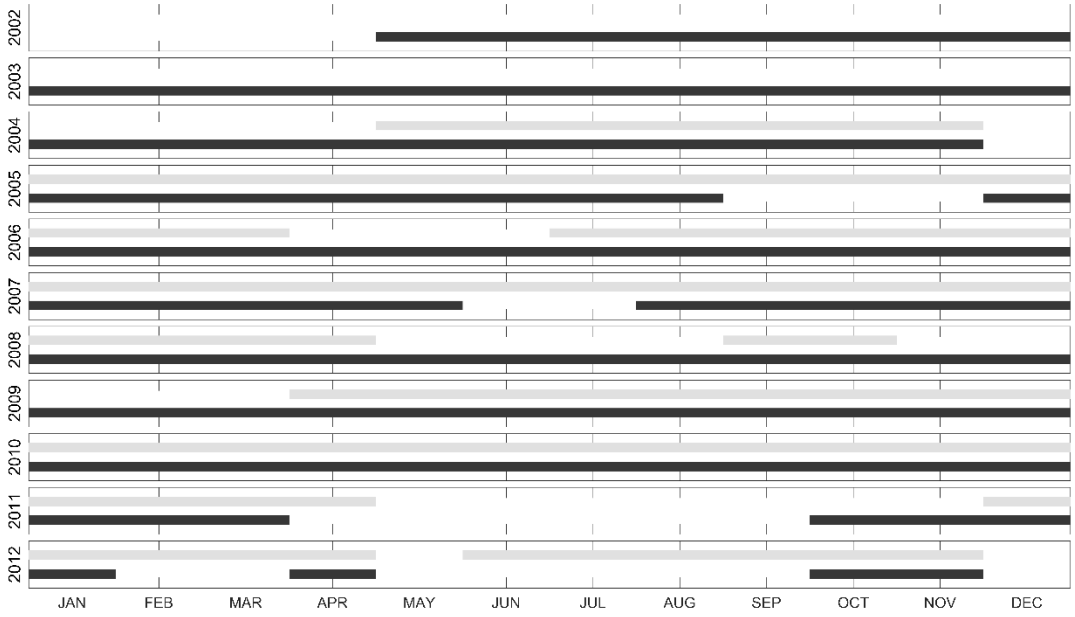
2002
2003
2004
2005
2006
2007
2008
2009
2010
2011
2012
JAN
FEB
MAR
APR
MAY
JUN
JUL
AUG
SEP
OCT
NOV
DEC

Figure 2.

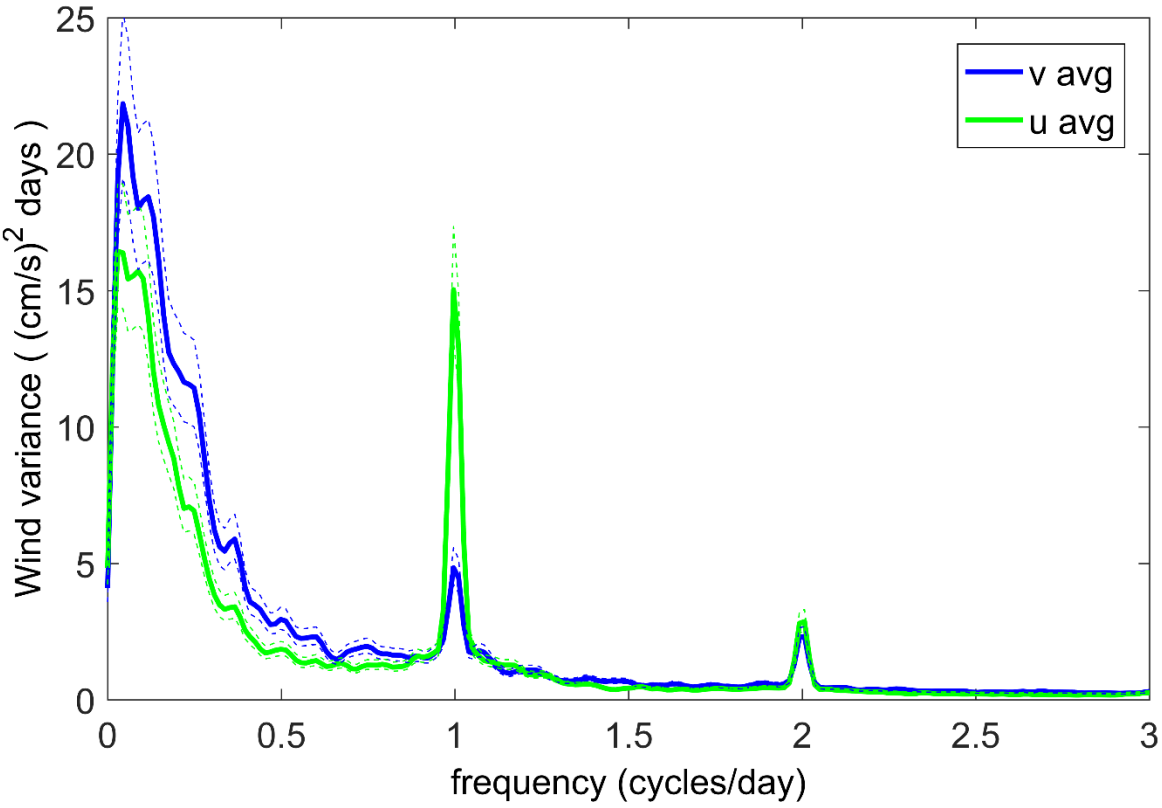
v avg
u avg
Wind variance ((cm/s)^2 days)
frequency (cycles/day)
0
5
10
15
20
25
0
0.5
1
1.5
2
2.5
3

Figure 3

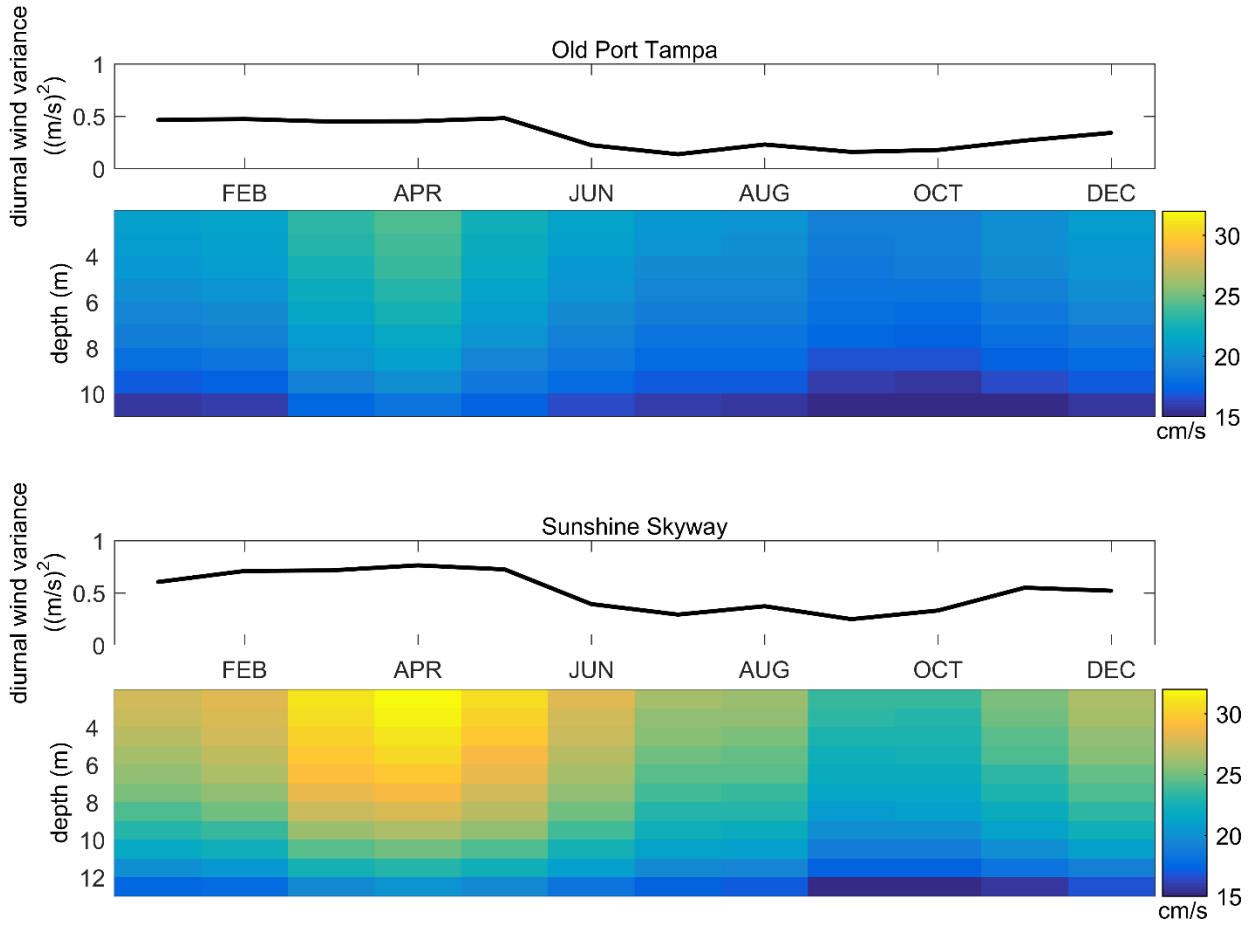
Old Port Tampa
diurnal wind variance ((m/s)^2)
1
0.5
0
FEB
APR
JUN
AUG
OCT
DEC
depth (m)
4
6
8
10
30
25
20
15
cm/s
Sunshine Skyway
diurnal wind variance ((m/s)^2)
1
0.5
0
FEB
APR
JUN
AUG
OCT
DEC
depth (m)
4
6
8
10
12
30
25
20
15
cm/s

Figure 4.

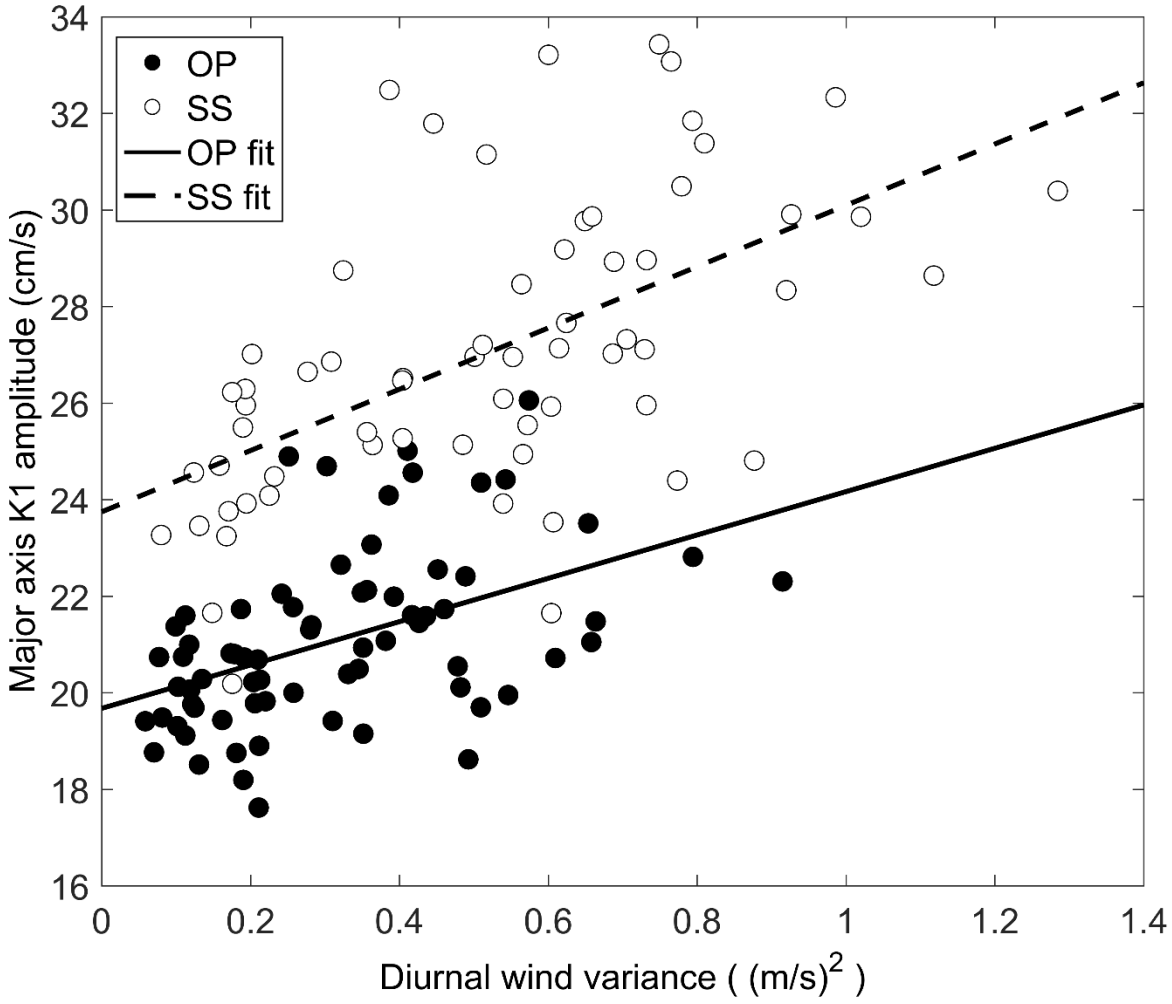
OP
SS
OP fit
SS fit
Major axis K1 amplitude (cm/s)
Diurnal wind variance ((m/s)^2)
34
32
30
28
26
24
22
20
18
16
0
0.2
0.4
0.6
0.8
1
1.2
1.4

Figure 5.

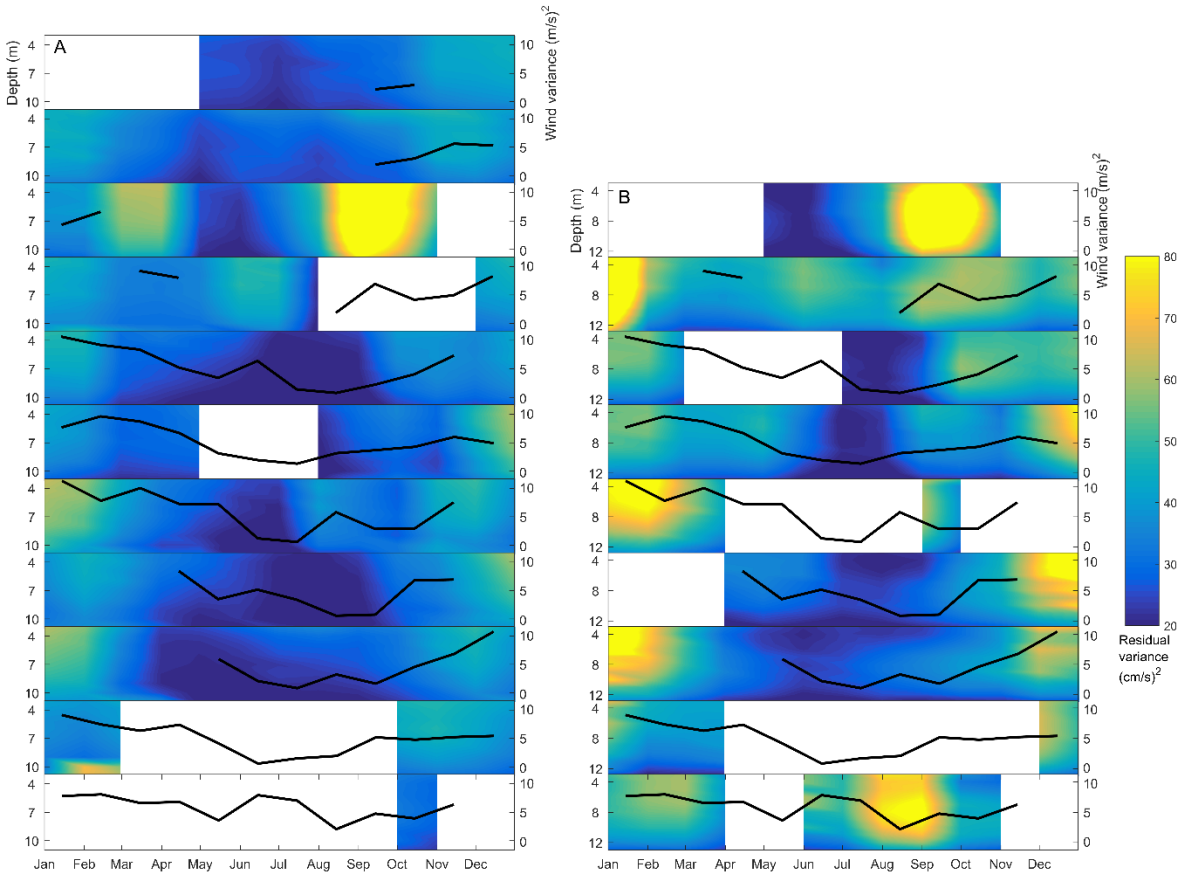
A
B
Depth (m)
Wind variance (m/s)^2
Residual variance (cm/s)^2
Jan
Feb
Mar
Apr
May
Jun
Jul
Aug
Sep
Oct
Nov
Dec

Figure 6.

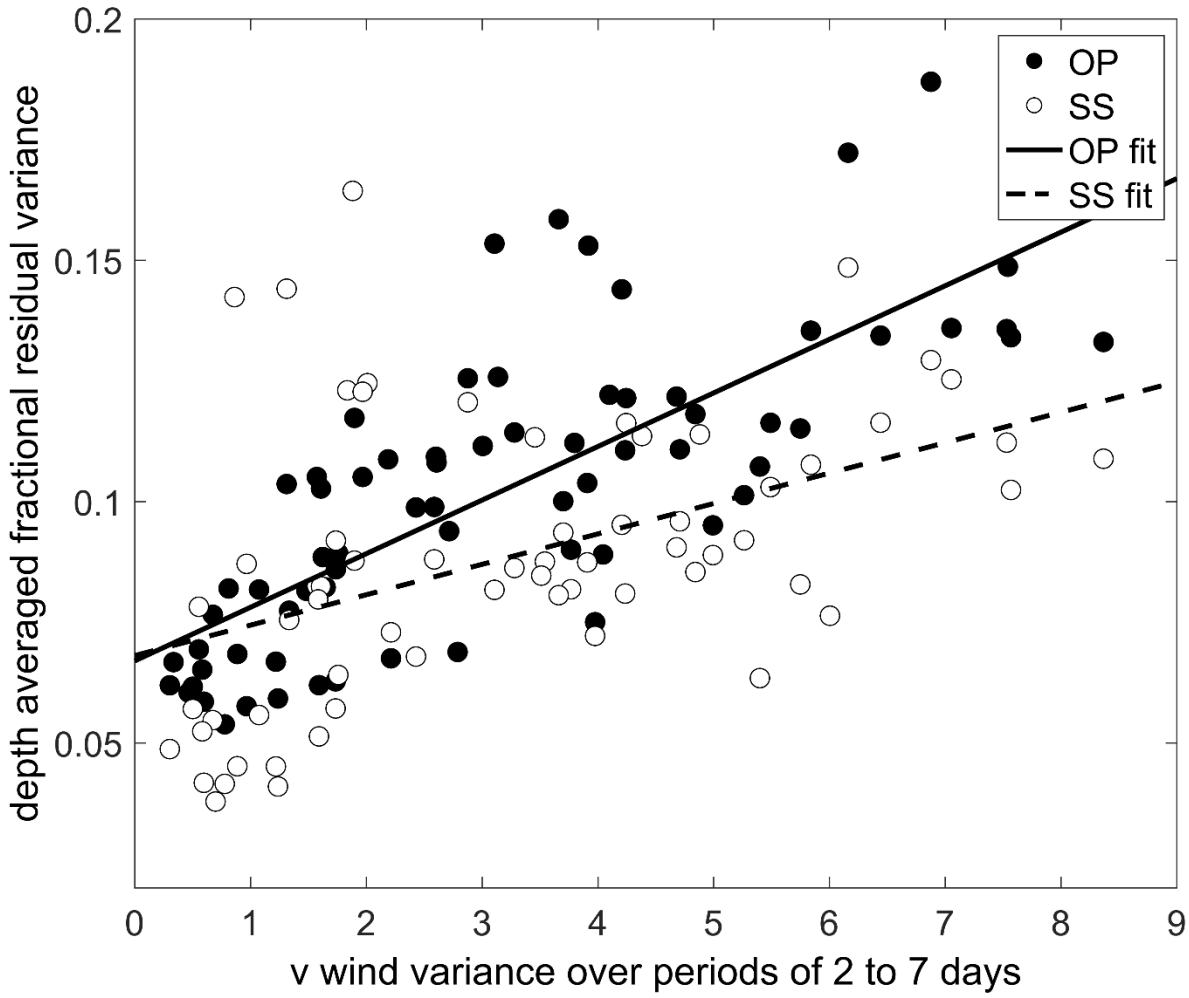
0.2
0.15
0.1
0.05
depth averaged fractional residual variance
0
1
2
3
4
5
6
7
8
9
v wind variance over periods of 2 to 7 days
OP
SS
OP fit
SS fit

Figure 7.

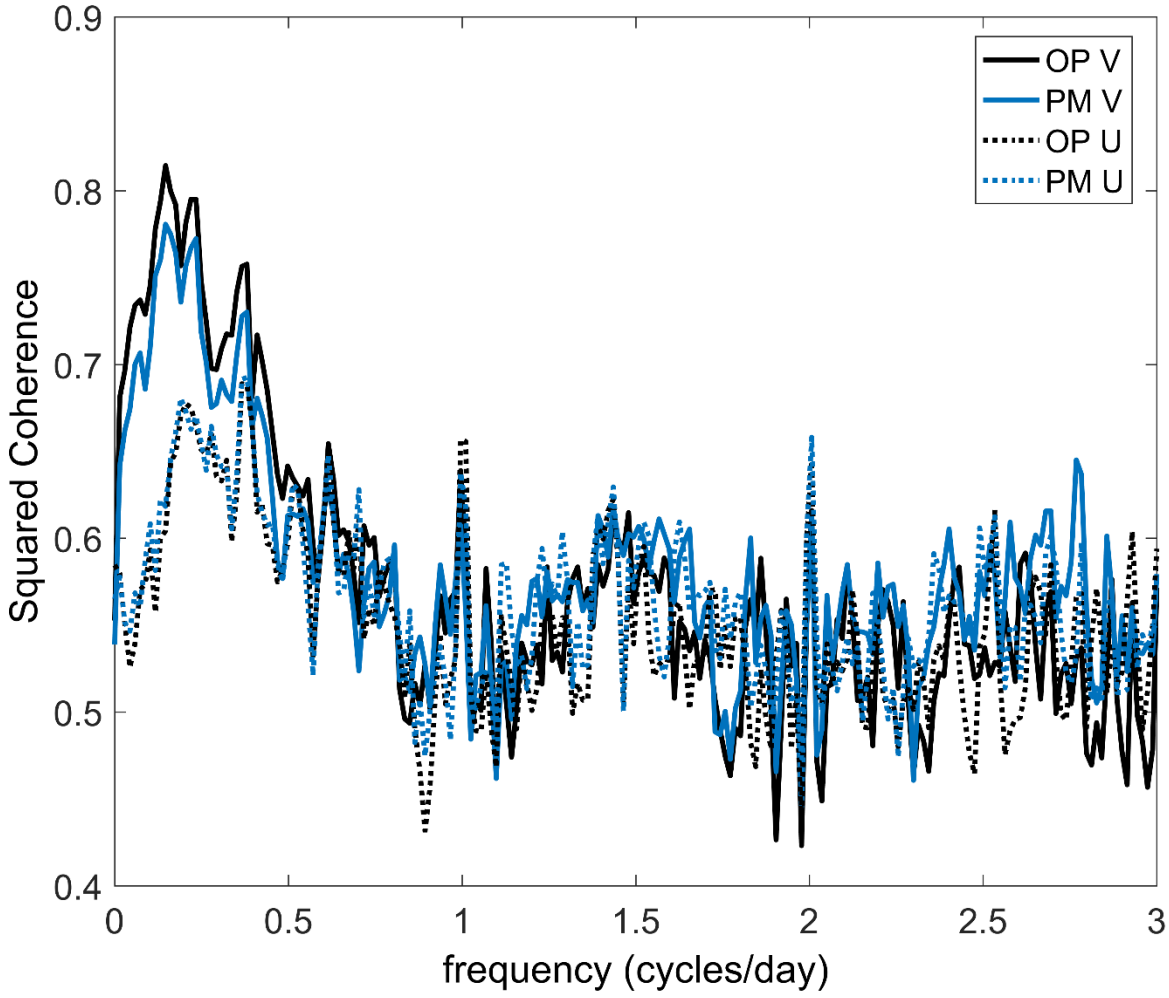
0.9
0.8
0.7
0.6
0.5
0.4
Squared Coherence
0
0.5
1
1.5
2
2.5
3
frequency (cycles/day)
OP V
PM V
OP U
PM U

Figure 8.

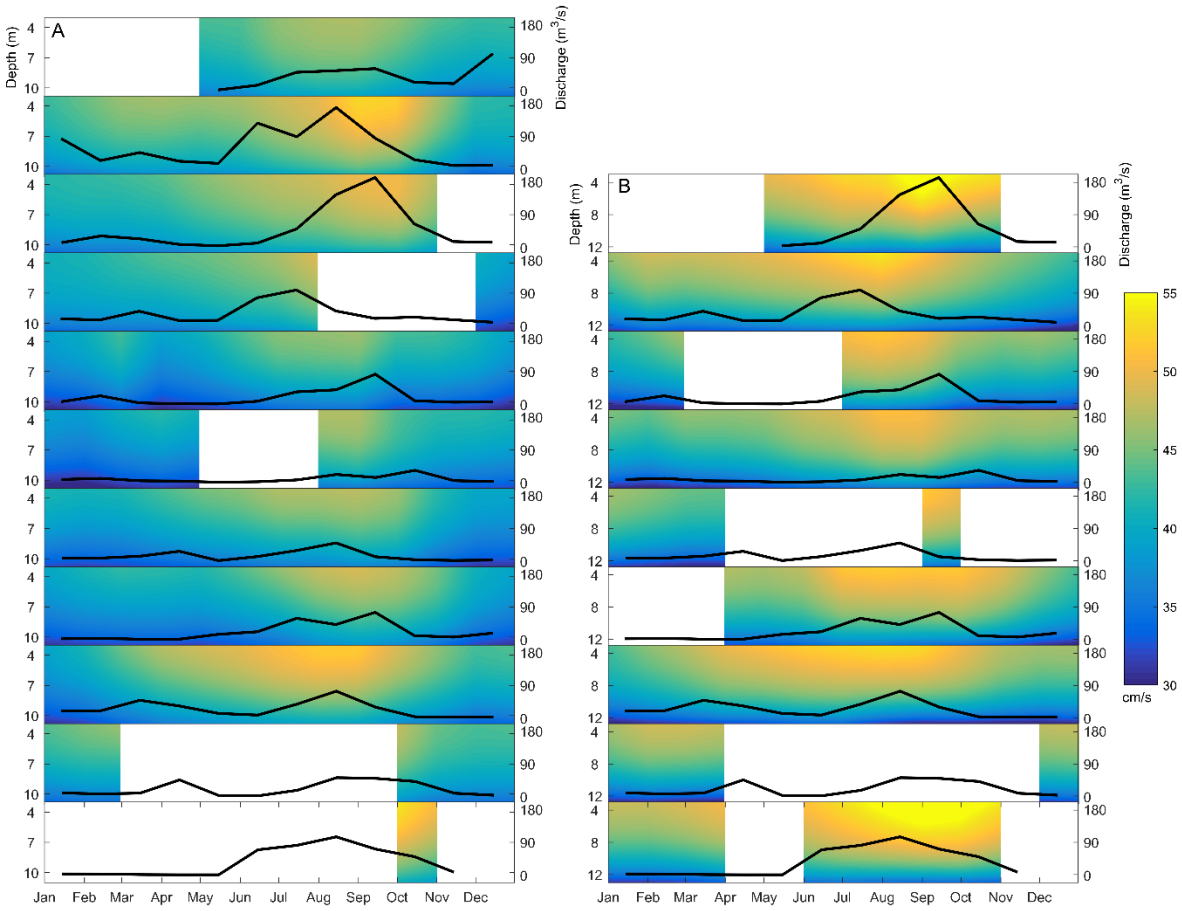
A
B
Depth (m)
Discharge (m3/s)
Jan
Feb
Mar
Apr
May
Jun
Jul
Aug
Sep
Oct
Nov
Dec
cm/s

Figure 9

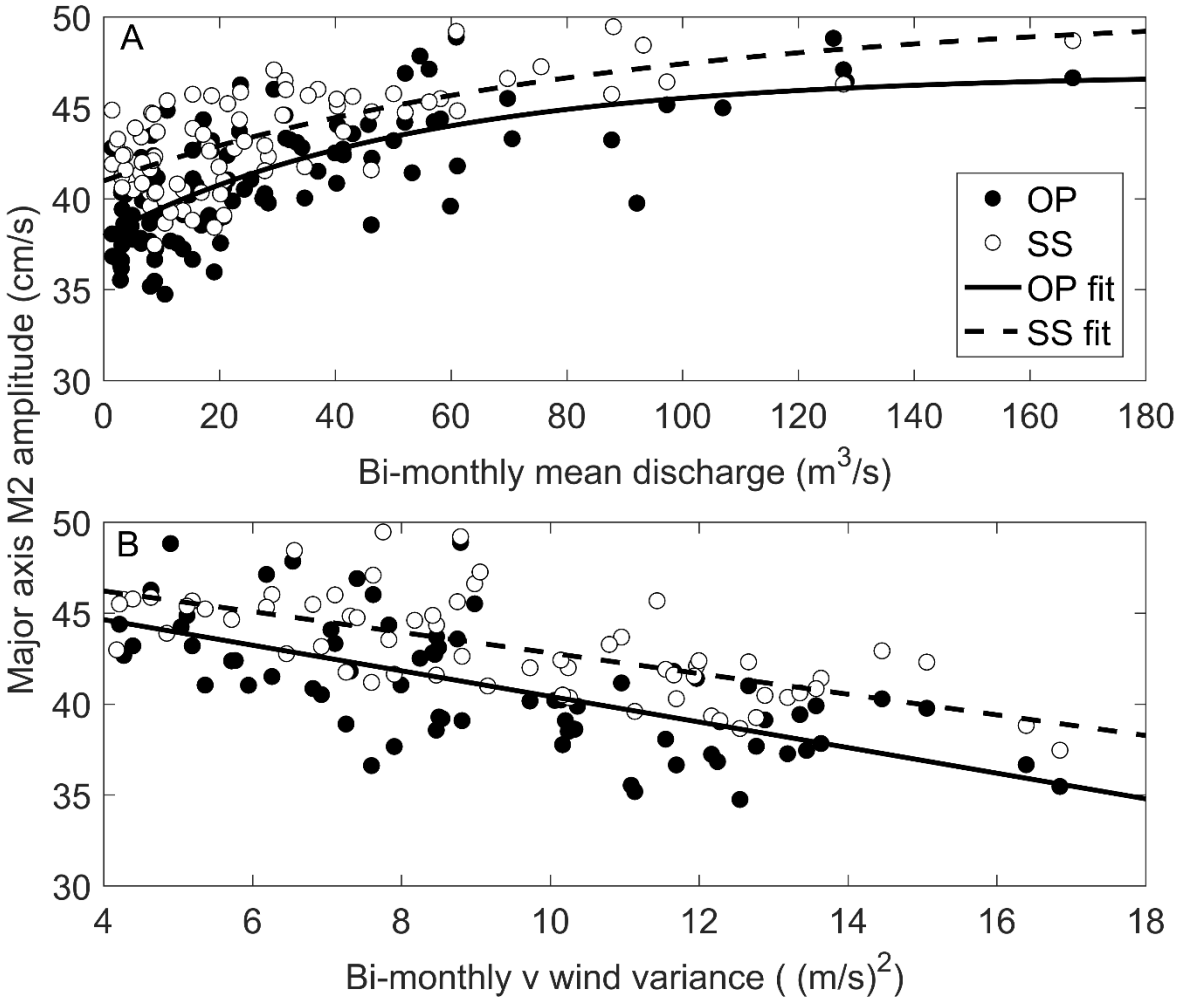
A
B
OP
SS
OP fit
SS fit
Major axis M2 amplitude (cm/s)
Bi-monthly mean discharge (m3/s)
Bi-monthly v wind variance ((m/s)2)
50
45
40
35
30
0
20
40
60
80
100
120
140
160
180
4
6
8
10
12
14
16
18

Figure 10.

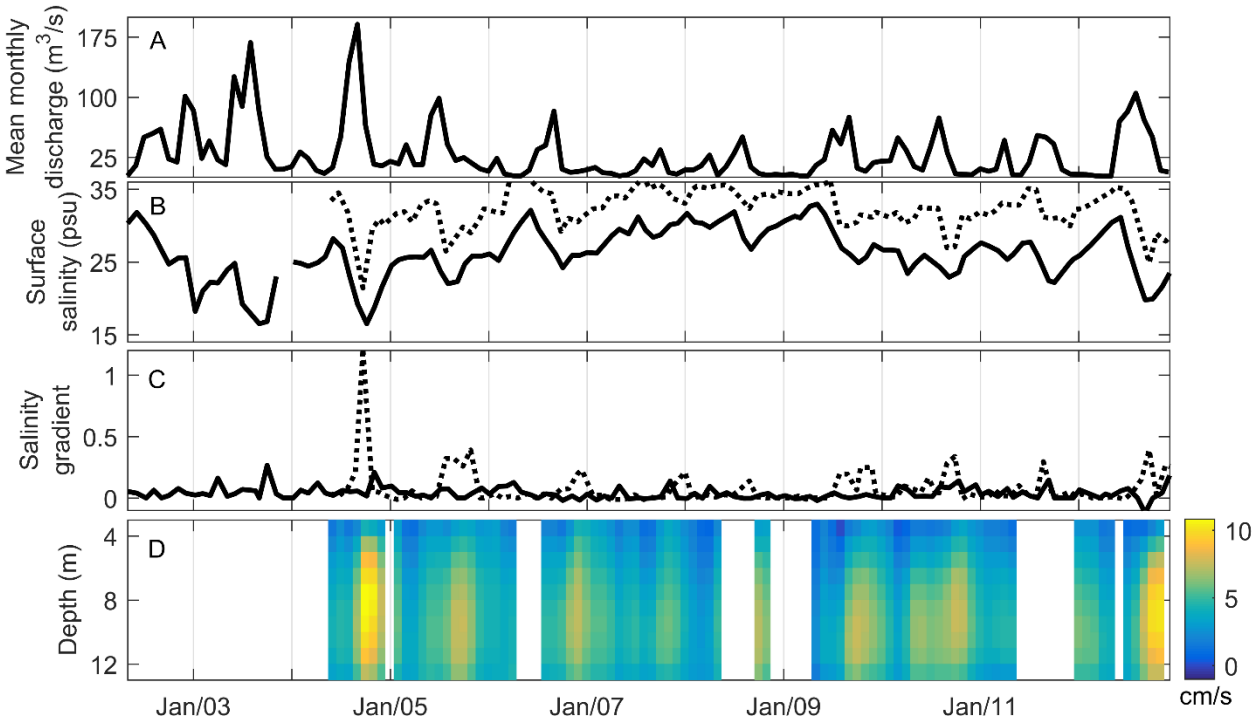
Mean monthly discharge (m3/s)
175
100
25
A
Surface salinity (psu)
35
25
15
B
Salinity gradient
1
0.5
0
C
Depth (m)
4
8
12
D
10
5
0
cm/s
Jan/03
Jan/05
Jan/07
Jan/09
Jan/11

Figure 11.

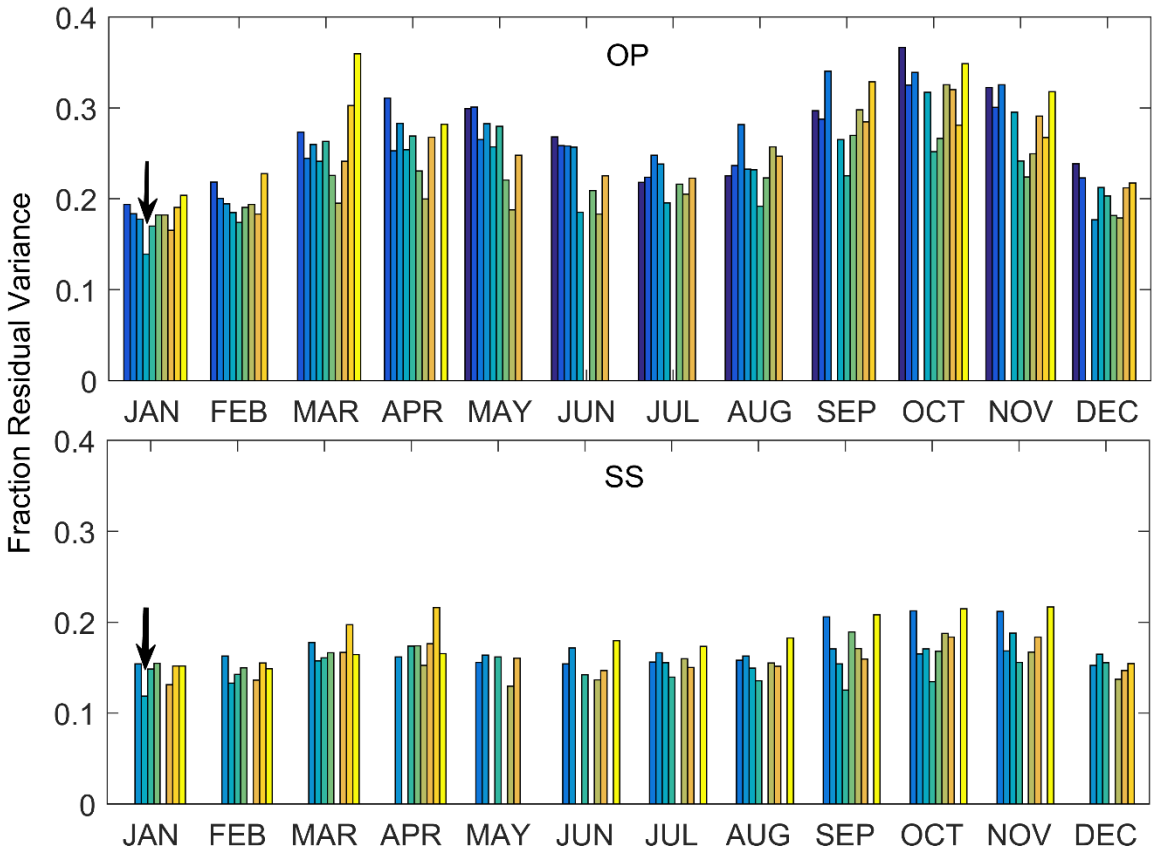
Fraction Residual Variance
OP
SS
0.4
0.3
0.2
0.1
0
JAN
FEB
MAR
APR
MAY
JUN
JUL
AUG
SEP
OCT
NOV
DEC

Figure 12.